Recent results on Standard Model physics from CMS

Nataša Raičević

on behalf of the CMS Collaboration

University of Montenegro, Faculty of Science and Mathematics

12th International Congress of the BPU

Bucharest, Romania, July 8–12, 2025

High precission measurements of the Standard Model

- ❑ High-precision measurements of the Standard Model are one of the cornerstones of modern particle physics

- ➢ Search for new physics via deviations
- ➢ Test the internal consistency of the Standard Model
- ➢ Improve and constrain Standard Model parameters
- ➢ Set limits on new physics scales
- ➢ Provide essential inputs for other experiments

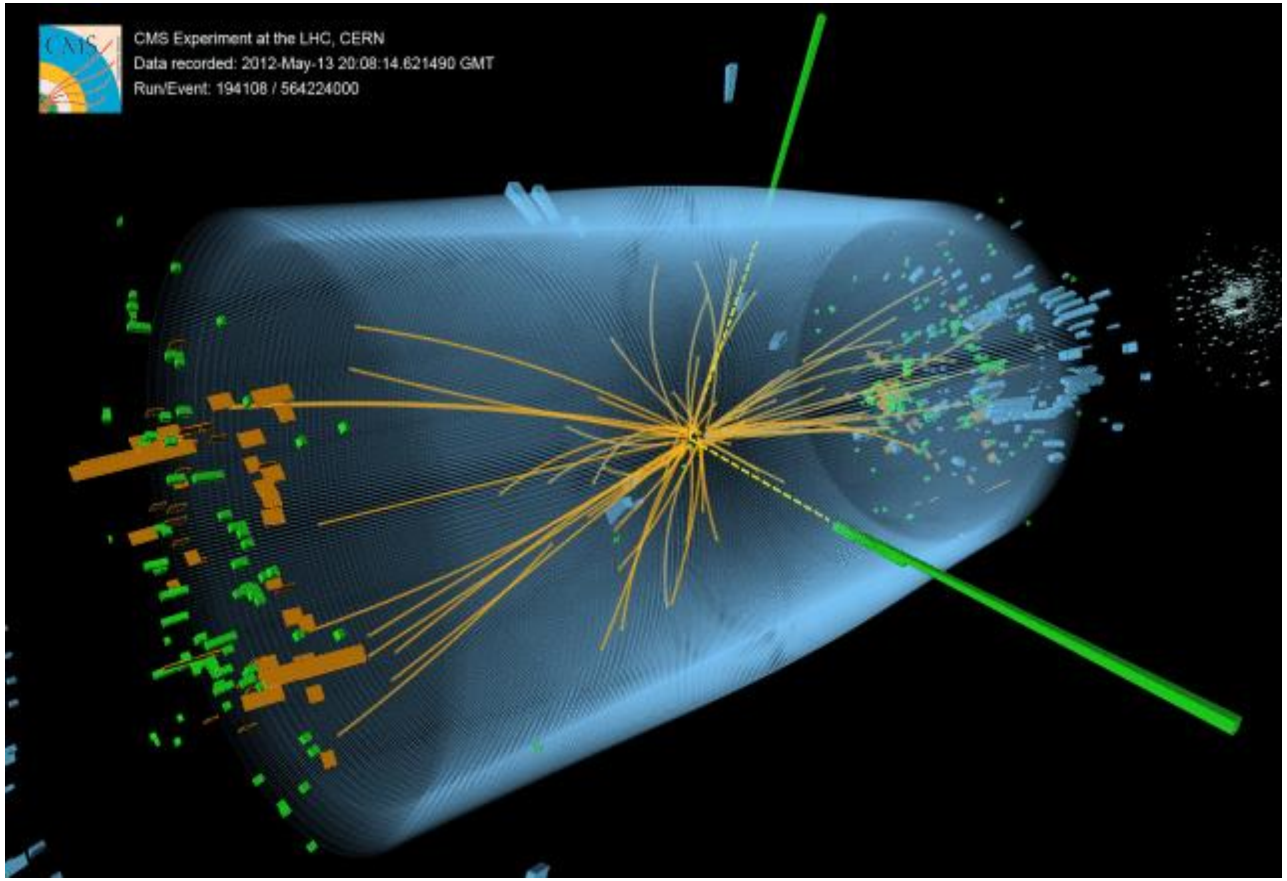

This talk focuses on recent CMS measurements in:

- ❑ QCD at the highest energies
- ❑ Electroweak phyiscs through multiboson production

Production of vector bosons (covered by I. Bubanja)

QCD at the highest energies

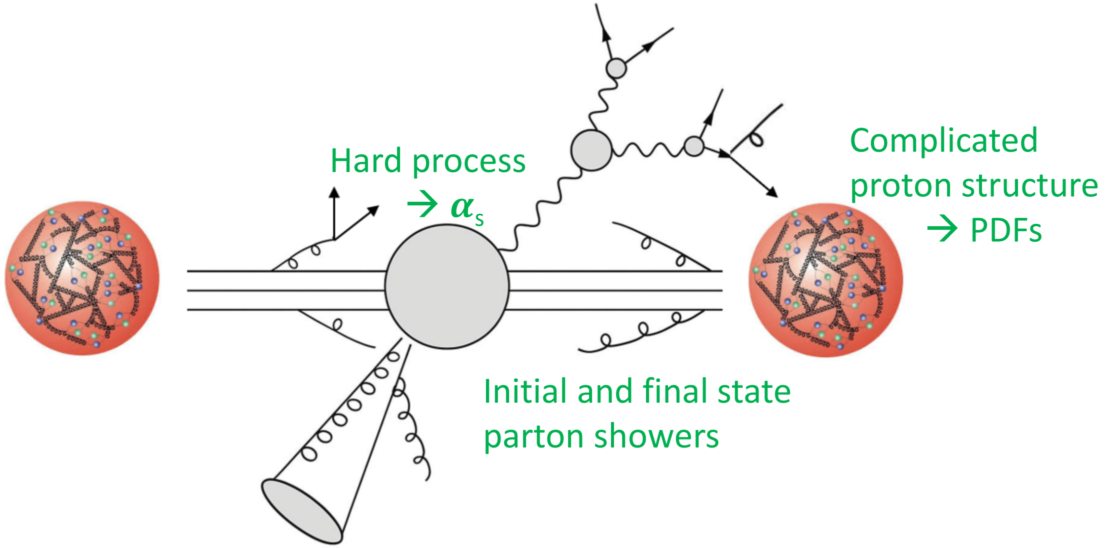

QCD measurements essential for:

- Determining the strong coupling and describing its running behaviour
- Determining parton distribution functions (PDFs)
- Modeling hard interactions
- Modeling soft processes

Recent results from CMS presented in this talk

+ Describing and modeling the evolution of parton showers in the initial and final state
+ Describing hadronisation and fragmentation processes
+ MPI, Beam remnants and the UE

Extracted α_s - PDG

PRD 110 (2024) 030001

NLO

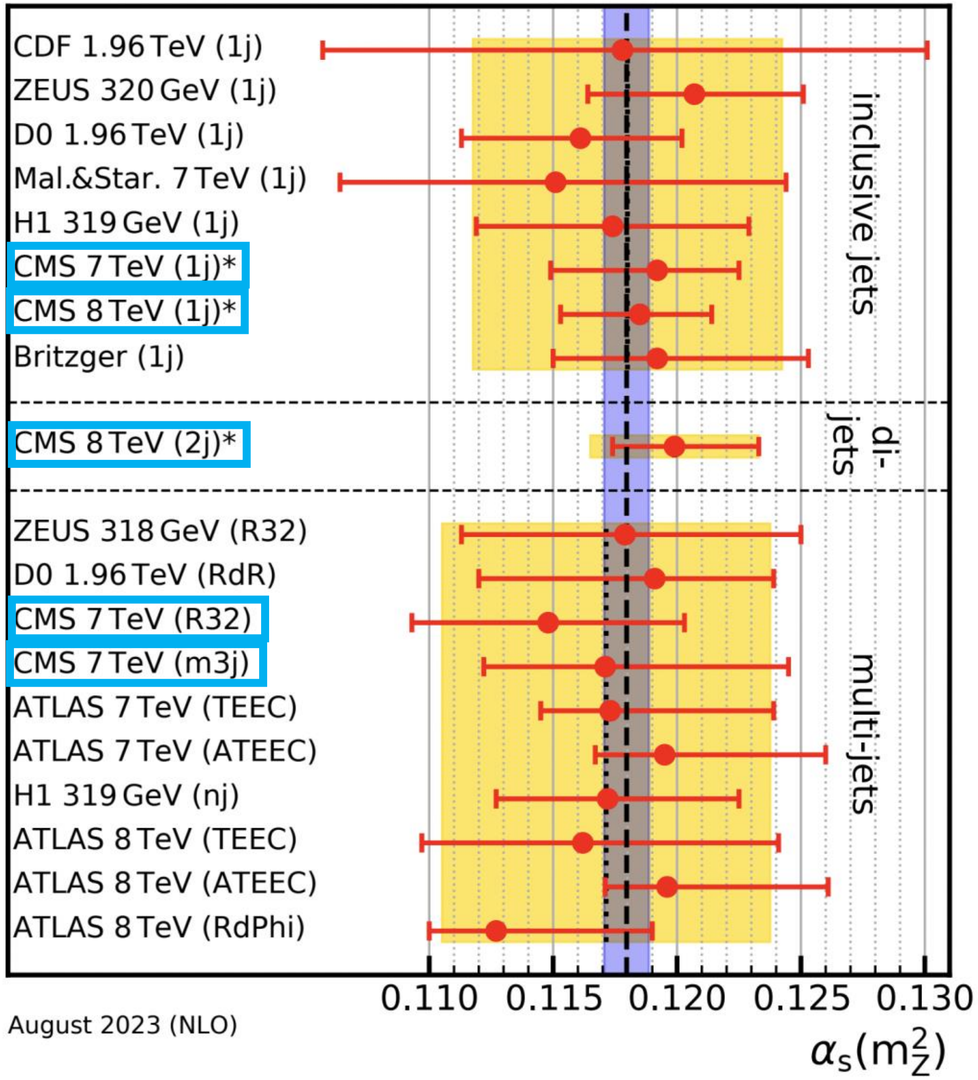

α_s determined from several CMS measurements

NNLO

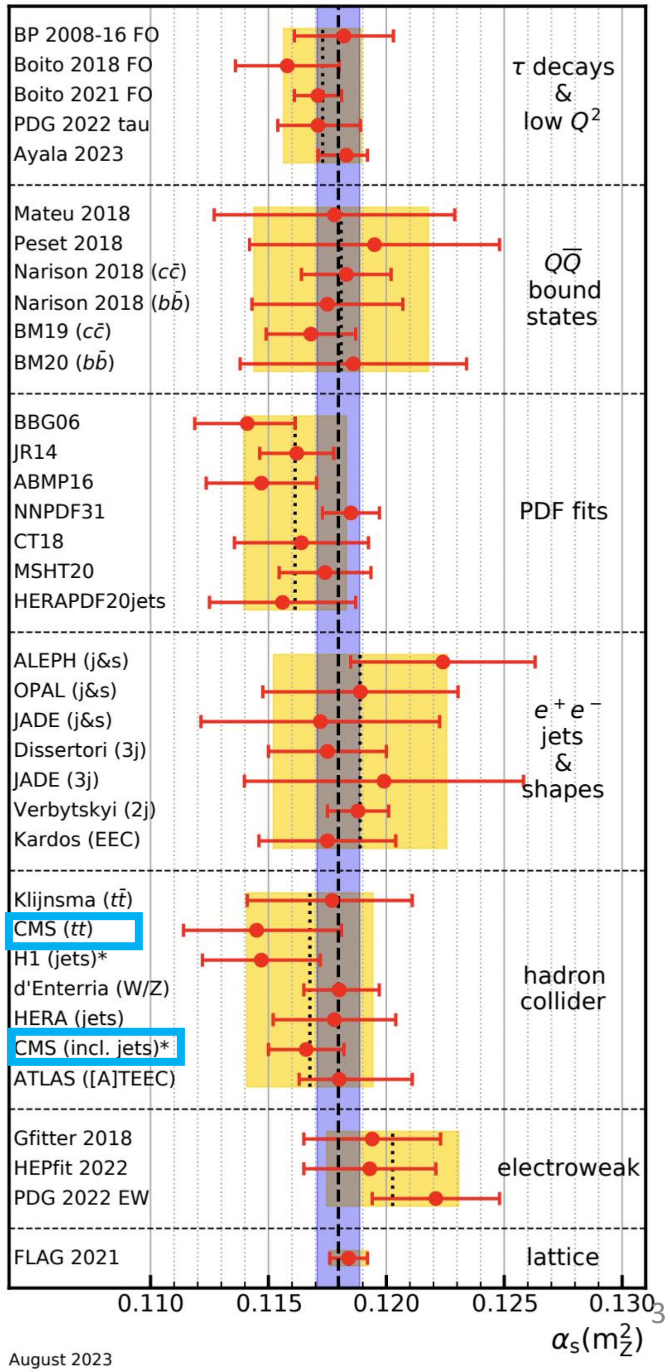

α_s from the simultenious fit with PDFs – NNLO QCD analysis

CMS-PAS-SMP-24-007 (Submitted to PLB)

- From inclusive jet production in proton-proton collisions at centre-of-mass energies of 2.76, 7, 8, and 13 TeV

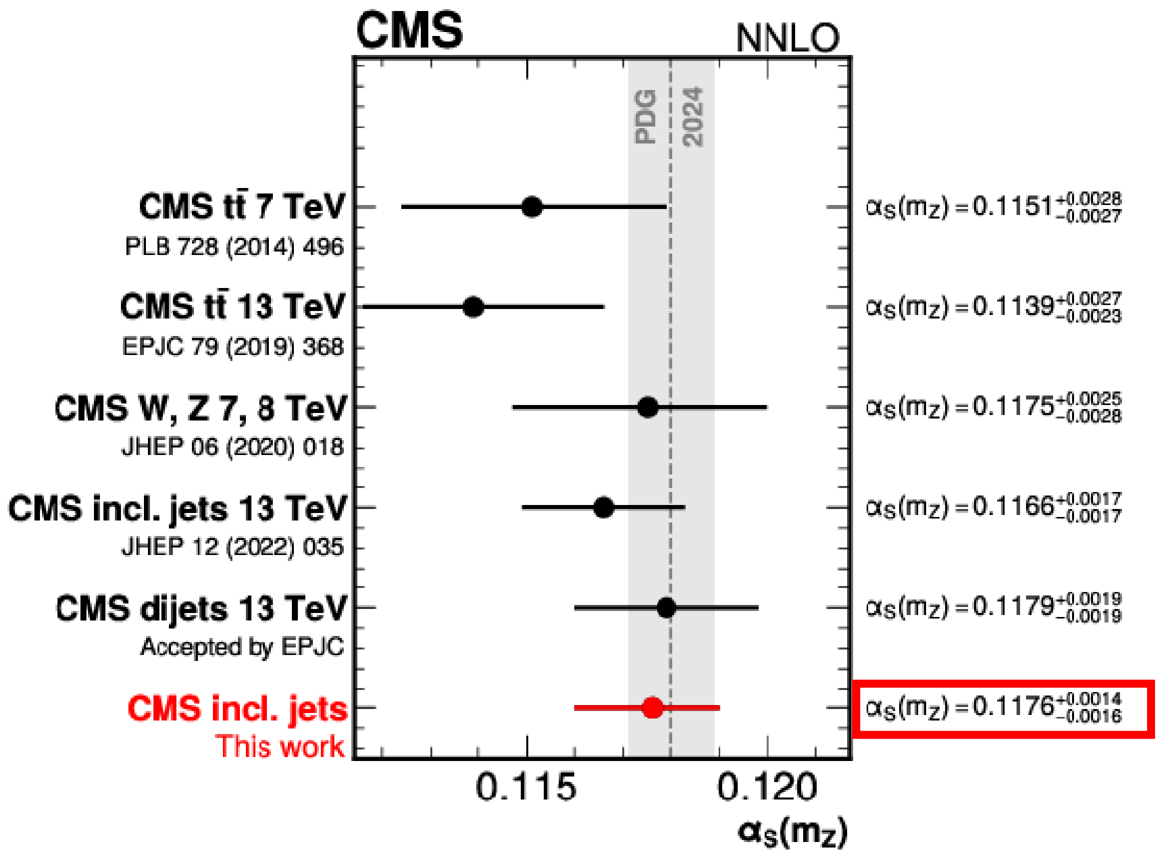

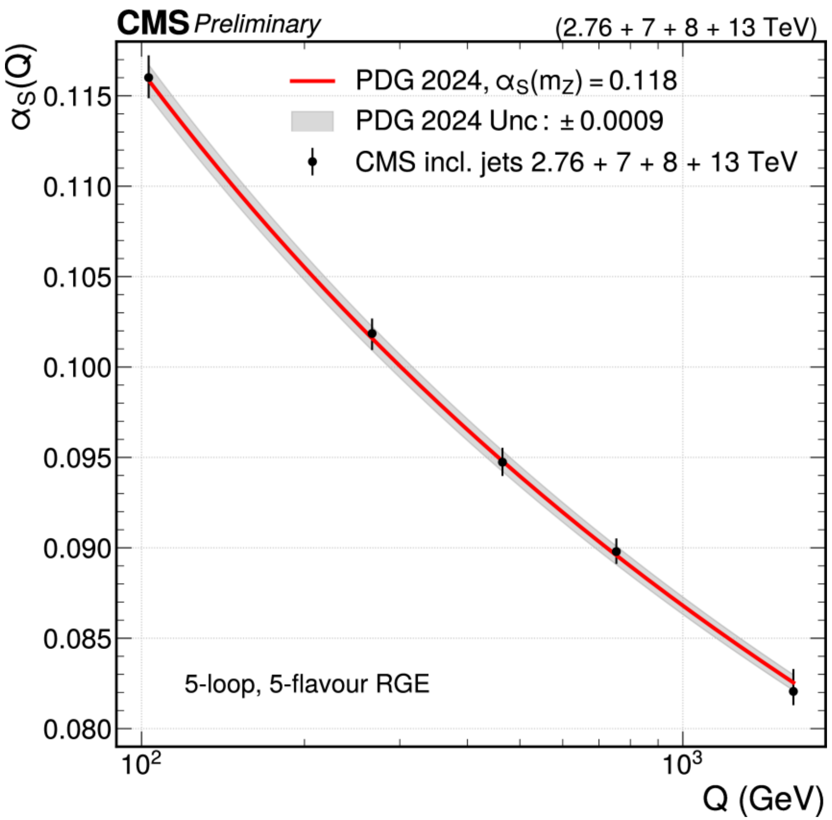

- Data from multiple center-of-mass energies improves precision by significantly reducing the fit uncertainty
- The dominant contribution to the uncertainty arises from missing higher order corrections
- The running of α_S as a function of the energy scale demonstrated at NNLO up to 1.6 TeV

PDFs from the simultenious fit with α_s

CMS-PAS-SMP-24-007 (Submitted to PLB)

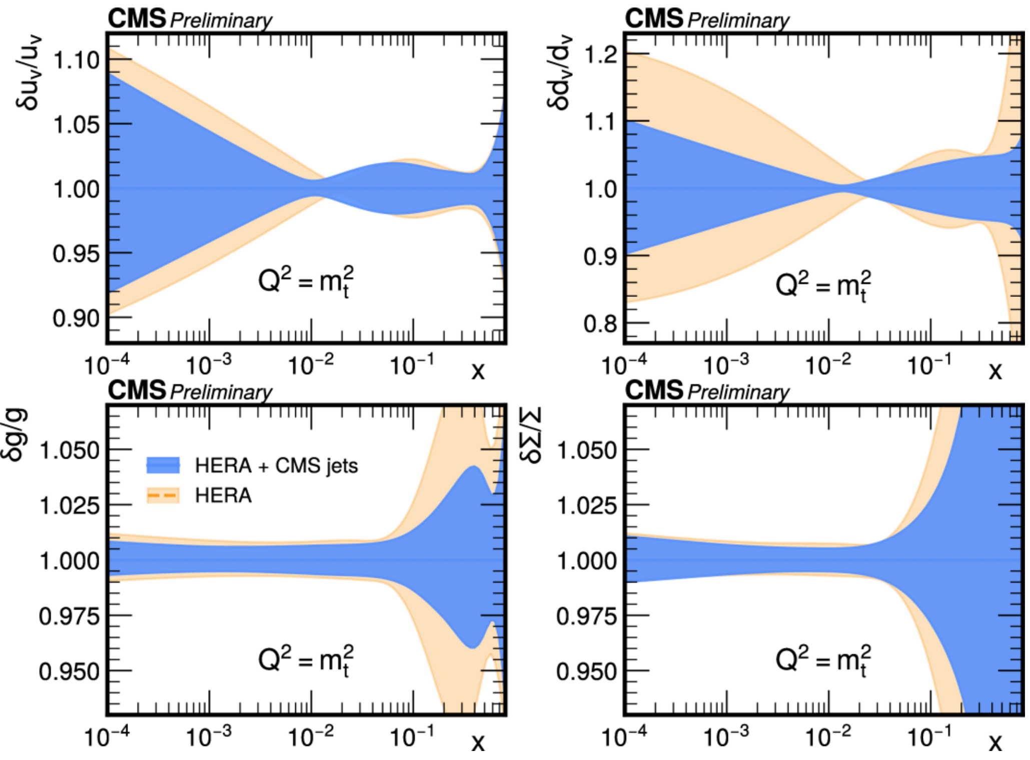

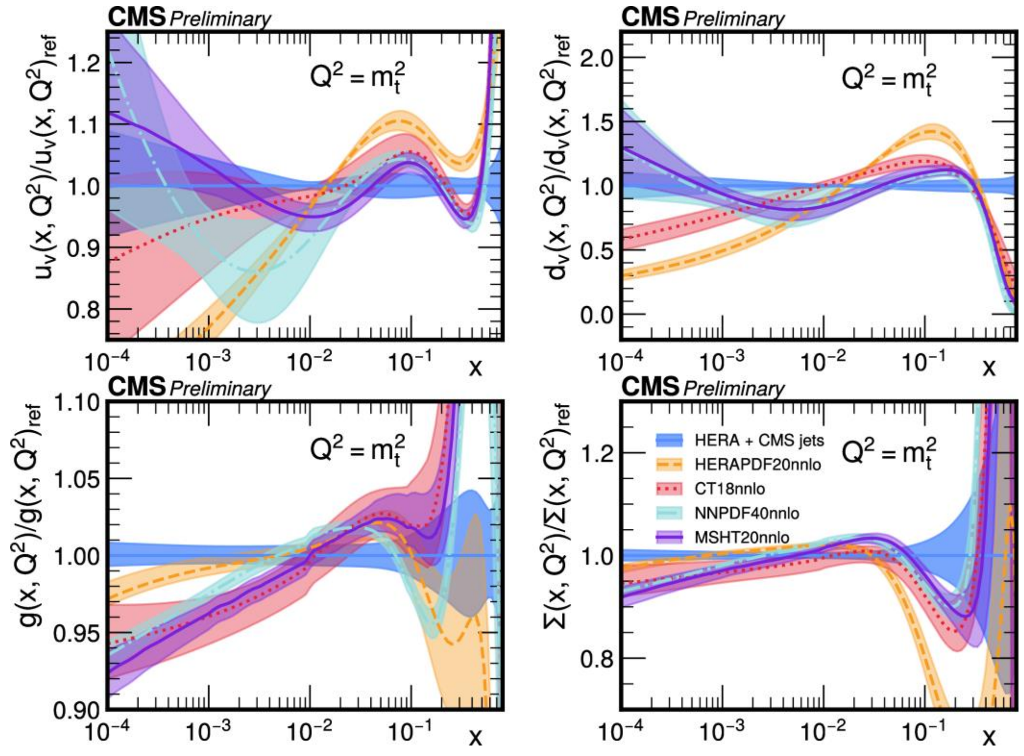

- Improvement in the uncertainties of all PDFs is observed by inclusion of CMS jet measurements in the QCD analysis.
- The inclusion of all available CMS inclusive jet measurements at different √s provides significant constraints on the valence d distribution

- By adding the CMS jet data → the valence PDF, in particular the d valence distribution, is observed to shift with respect to HERAPDF20 towards the results of the global PDFs

The uncertainties are given at 68% CL

Event Shape (ES) variables from jets at 13 TeV

CMS-PAS-SMP-22-004 (Public since April 2025)

- ESV using charged particles inside jets in proton-proton collisions – 138 pb^{-1}

  - Sensitive to the perturbative part of hadron collisions as well as to the energy flow in the final state of a high energy collision event

  - Minimize impact of systematic uncertainties

- Measured variables designed to have higher values for multijet, spherical events and lower values for back-to-back two-jet events

  - Complement of transverse thrust, $\tau_{\perp}$ - more dependent on the initial hard scattering

  - Third-jet resolution parameter, Y_{23} - sensitive to the clustering and substructure of the jets

  - Jet Broadening, $B_T \equiv B_U + B_L$

  - Jet masses, $\rho_{Tot} \equiv \rho_U + \rho_L$

  depend more on the subsequent nonperturbative part of QCD, i.e., the evolution of the partons into the final state particles

- This is the first CMS study that uses charged particles inside jets to evaluate ESV

- For each variable, detector effects are corrected using a two-dimensional unfolding in which the average p_T of the leading and the second leading jets in events, $H_{T,2} = ½(p_{T,j1} + p_{T,j2})$, and variables are unfolded simultaneously

- $\tau_\perp$ and ρ^T_{Tot} use the momenta of the particles in the transverse plane (p_T) and ρ_{Tot}, B_T , and Y_{23} use the complete momentum information

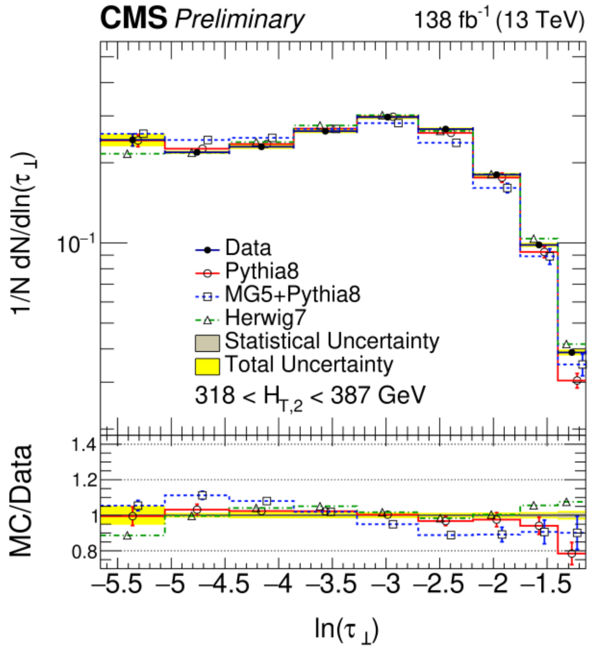

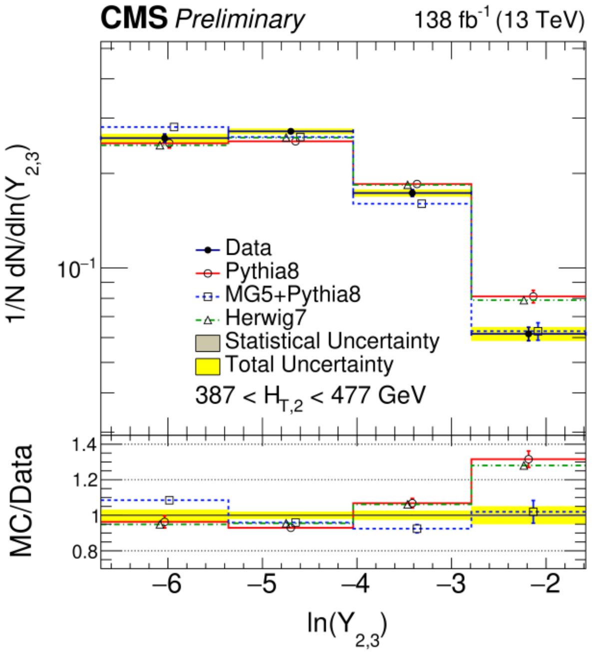

- General trend:

- the predictions of PYTHIA 8 and HERWIG 7, show good agreement with data for $\tau_\perp$ and ρ^T_{Tot}, but overestimate multijet events for ρ_{Tot}, B_T , and Y_{23}.

  → Indicates that the modelling of fragmentation and hadronization needs to be examined

- MG5+PYTHIA 8 underestimates multijet spherical events except for Y_{23}

  → Possible issues in the combination of ME calculations with the PS

- There is room for improvement in QCD modelling and the understanding of energy flow

ES in minimum bias events at 13 TeV

[CMS-PAS-SMP-23-008]

- Minimum bias data (~1 inelastic proton-proton collision per bunch crossing) – integrated luminosity of 64 μb^{-1}
- Many new measurements highlight the need for additional experimental input to soft and nonperturbative QCD
- The kinematics of reconstructed tracks were used to unfold the distributions to the level of stable charged particles

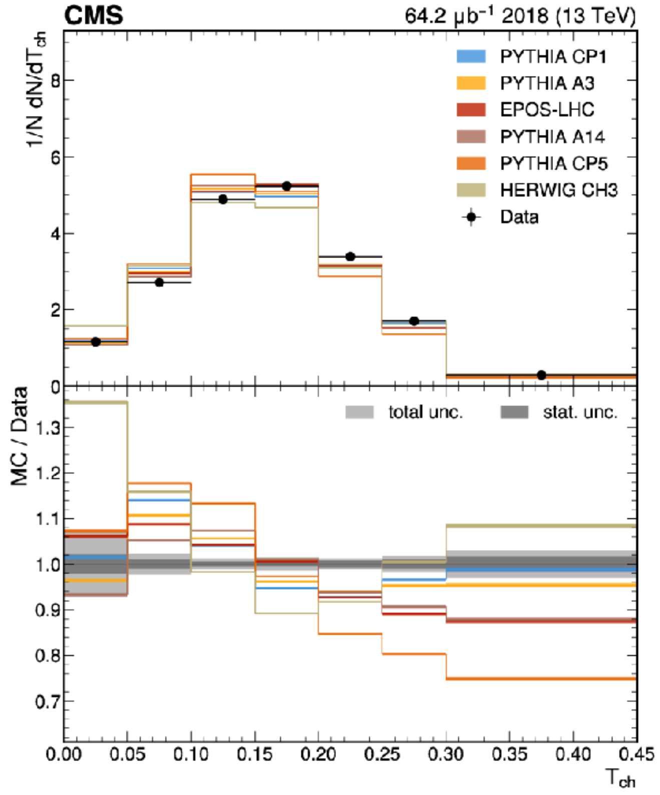

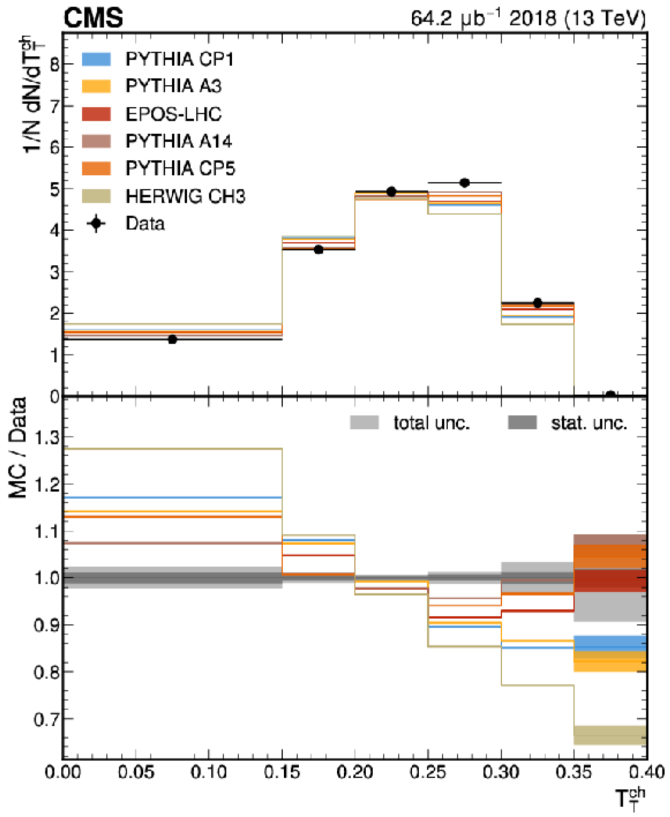

T ~ 0 – higly jet-like event (2 jet events)
T ~ 0.5 - isotropic

- 8 variables measured: charged particle multiplicity and invariant mass, isotropy, broadening, thrust and sphericity (also in the transverse plane)
- The difference between data and MC observed for all the variables
- General trend:
  Isotropy underestimated and anisotropy overestimated in the models – observed also in the transverse plane

→ Mismodeling not coming only from the poorly modelled longitudinal components

➢ Is poor modeling of event shapes coming from the distribution of the number of charged particles ?

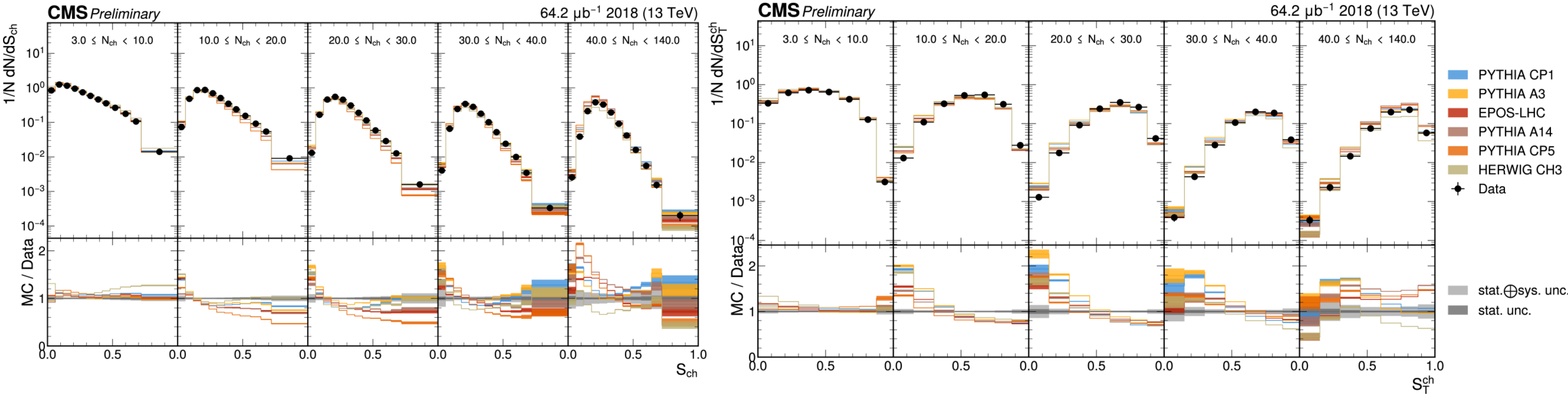

Sphericity S ~ 1 → isotropic

❑ Isotropy underestimated in different charged-particle multiplicity bins

→ The poor modeling of event shapes is likely not primarily due to the distribution of the number of charged particles

Electroweak multiboson interactions predicted in the SM

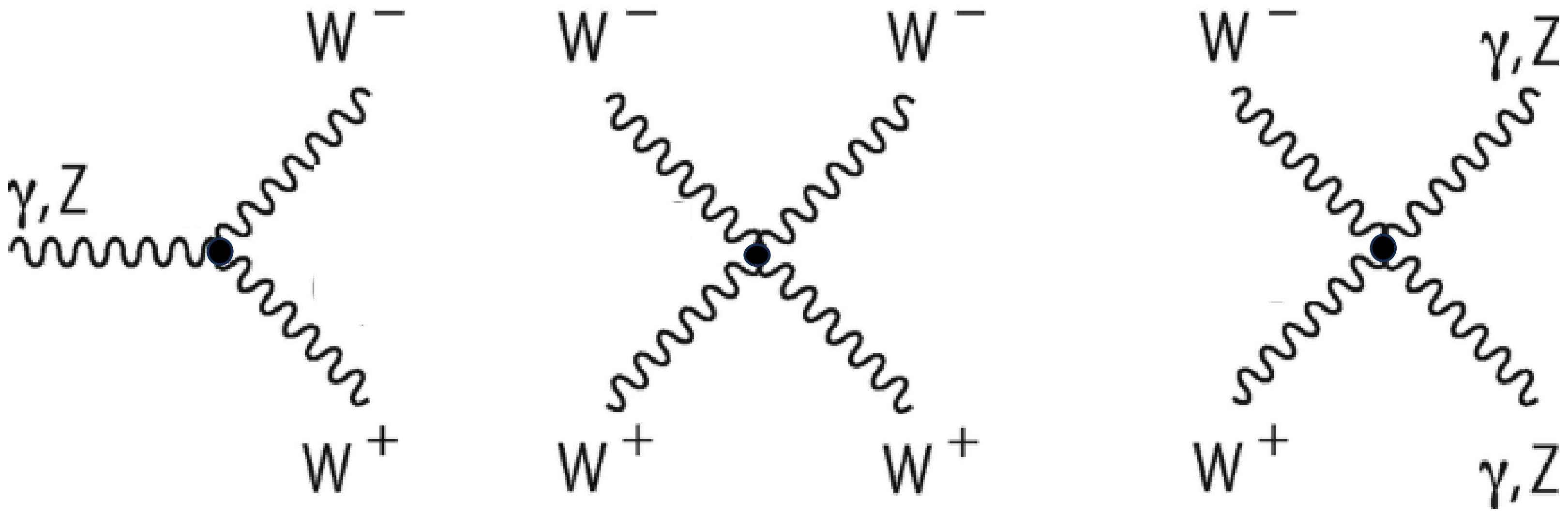

- ❑ Anomalous neutral triple/quatric gauge couplings → allowed in the presence of new physics
- ❑ Several of such heavy bosons produced together is a rare process

→ Multiboson production process great tool to:

- ➢ Test and study the SM expectations
- ➢ Study electroweak sector where one could search for a new physics impacting EWSB

Diboson Zγ at CMS at 13 TeV with full RUN 2 data

CMS-PAS-SMP-22-009

- Large production rate and clean signatures

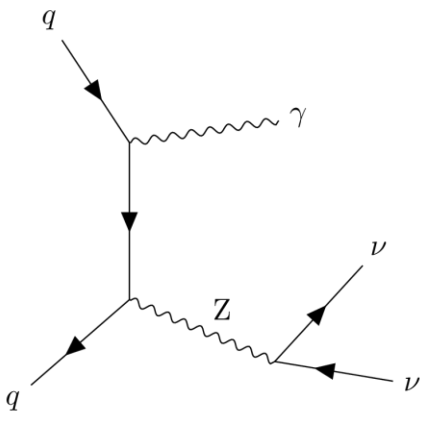

SM

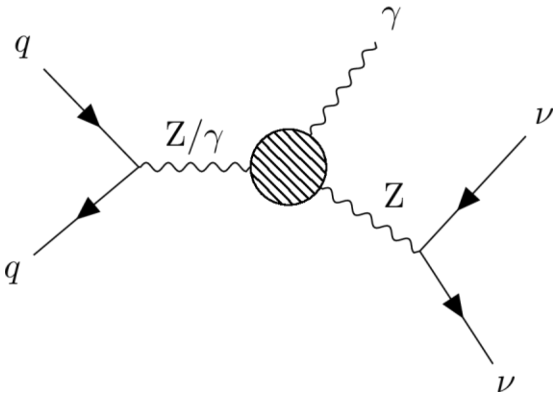

The BSM s-channel Zγγ production due to the presence of aNTGCs

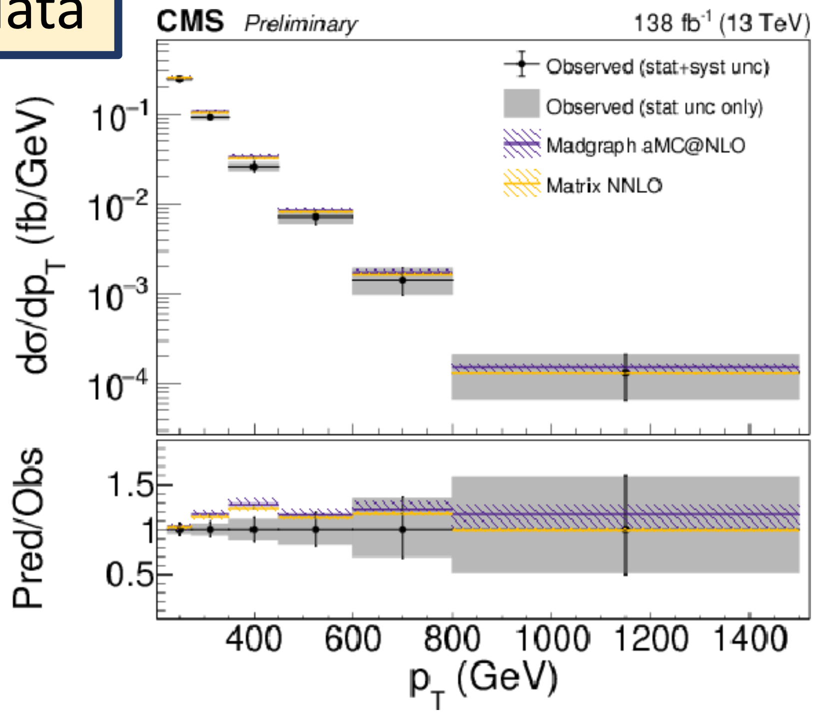

- The measured cross section is compatible with the theoretical predictions in QCD
- The study of the photon pT spectrum yields the most stringent limits on the aNTGC

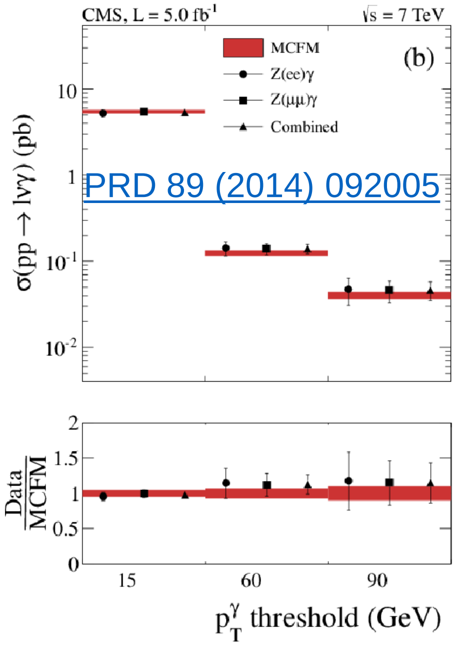

PRD 89 (2014) 092005

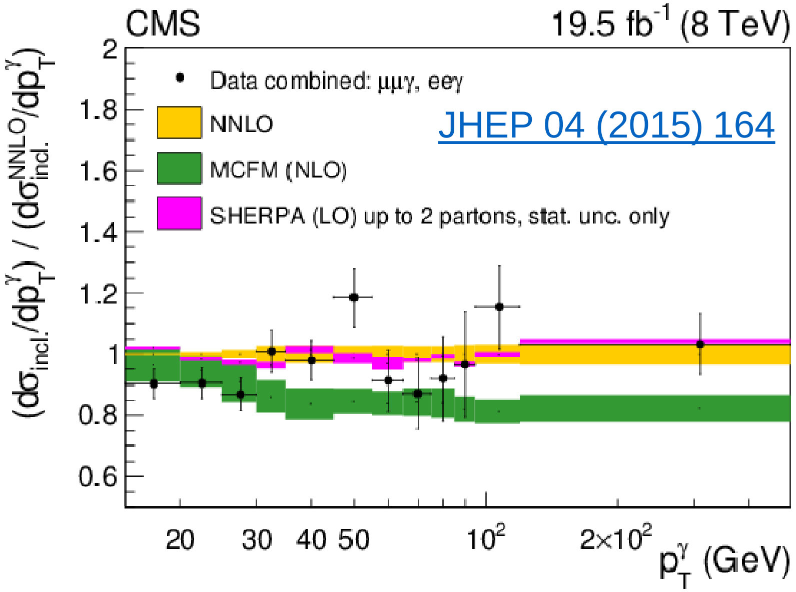

JHEP 04 (2015) 164

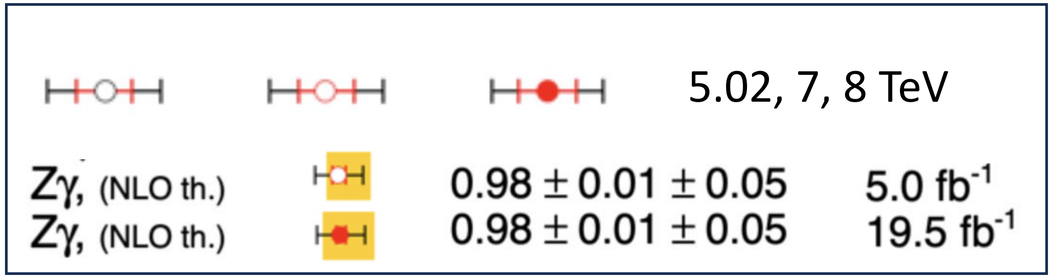

First measurement of $Z\gamma$ at 13.6 TeV

CMS-PAS-SMP-24-002 (Public since March 2025)

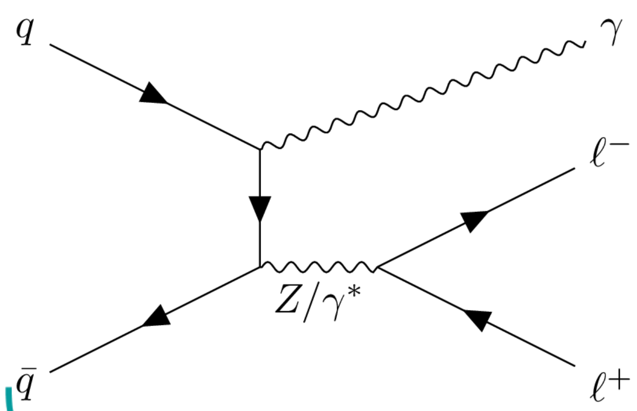

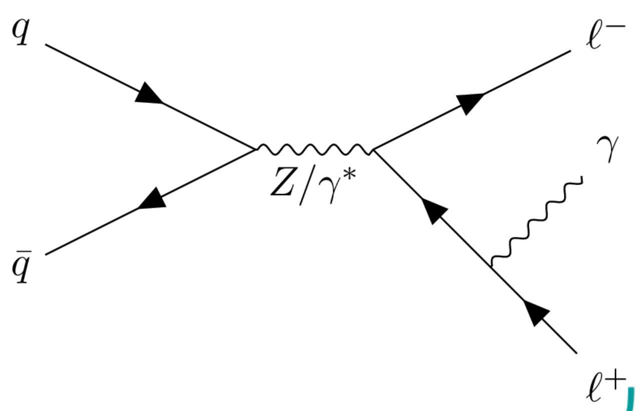

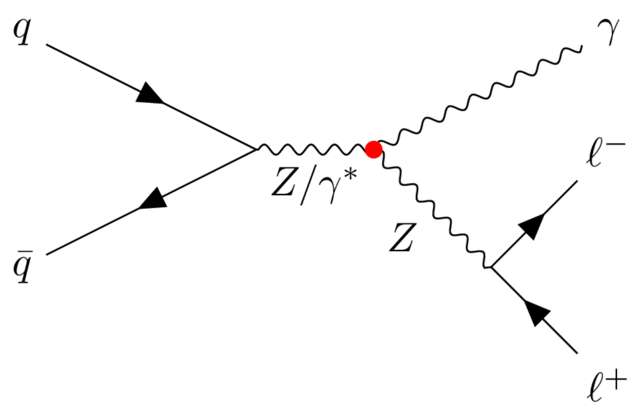

LO SM Feynman diagrams

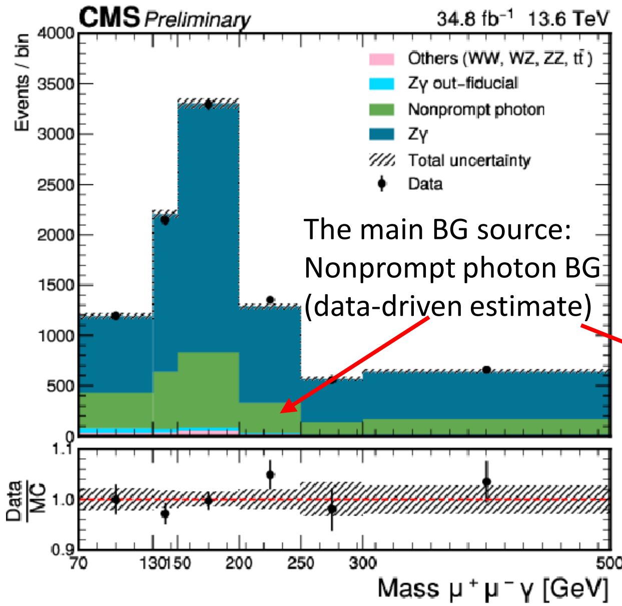

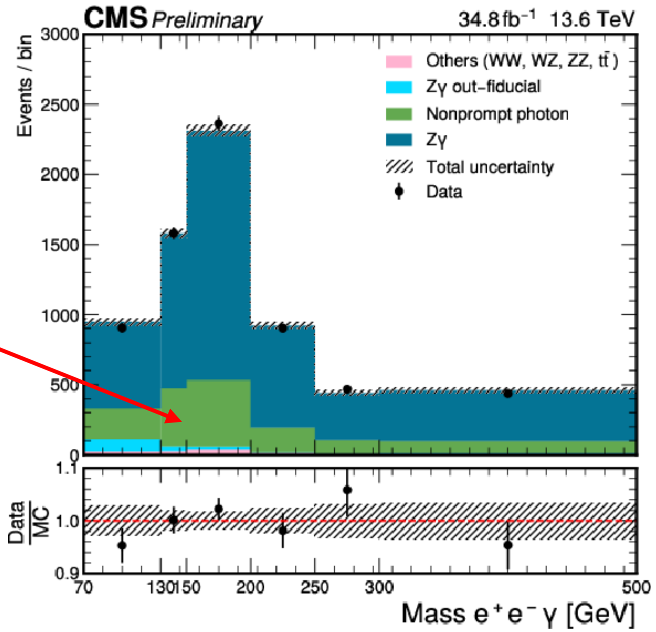

The main BG source:
Nonprompt photon BG
(data-driven estimate)

- Photon ID and luminosity are the leading uncertainties in the measurement

Channel	$\sigma \times BR(Z\gamma \to l^+l^-\gamma) \pm$ th. $\pm$ syst. $\pm$ stat. (pb)
predicted $Z\gamma$ ($\mu\mu$)	$0.961 \pm 0.004 \pm 0.028 \pm 0.019$
predicted $Z\gamma$ (ee)	$0.961 \pm 0.004 \pm 0.037 \pm 0.021$
predicted $Z\gamma$ (combined)	$1.922 \pm 0.006 \pm 0.056 \pm 0.033$
observed $Z\gamma$ ($\mu\mu$)	$0.928 \pm 0.004 \pm 0.027 \pm 0.018$
observed $Z\gamma$ (ee)	$0.975 \pm 0.003 \pm 0.038 \pm 0.021$
observed $Z\gamma$ (combined)	$1.896 \pm 0.006 \pm 0.054 \pm 0.033$

→ Good agreement with NLO predictions from MadGraph

First ZZγ measurement with full RUN 2 data

CMS-PAS-SMP-24-014

SM

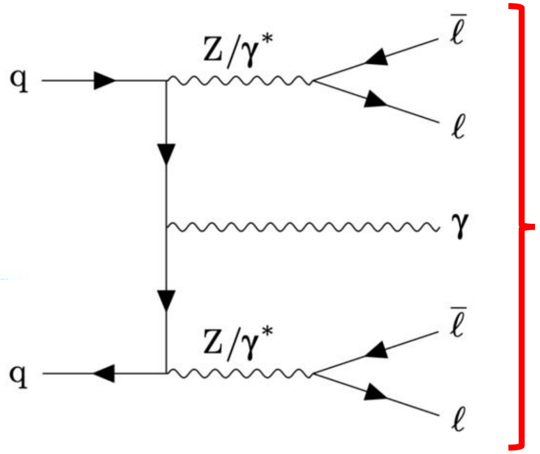

$4l + \gamma$

TEST

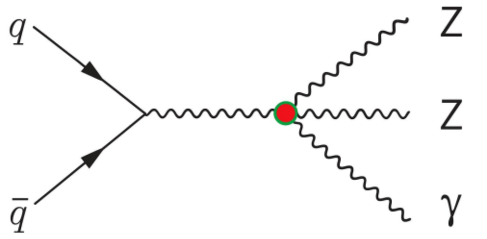

anomalous Quatric Gauge Couplings (aQGC)

- ❑ The signal region is affected by two types of reducible BGs:
- ➢ nonprompt leptons/photons estimated from data
- ➢ Significance in the inclusive measurement: observed 5.1 (expected 4.1) SD
- ❑ To distinguished from FSR, requiring inv. mass of the 2l + γ system to be above 100 GeV
- ➢ nonprompt photons (estimated from simulation)

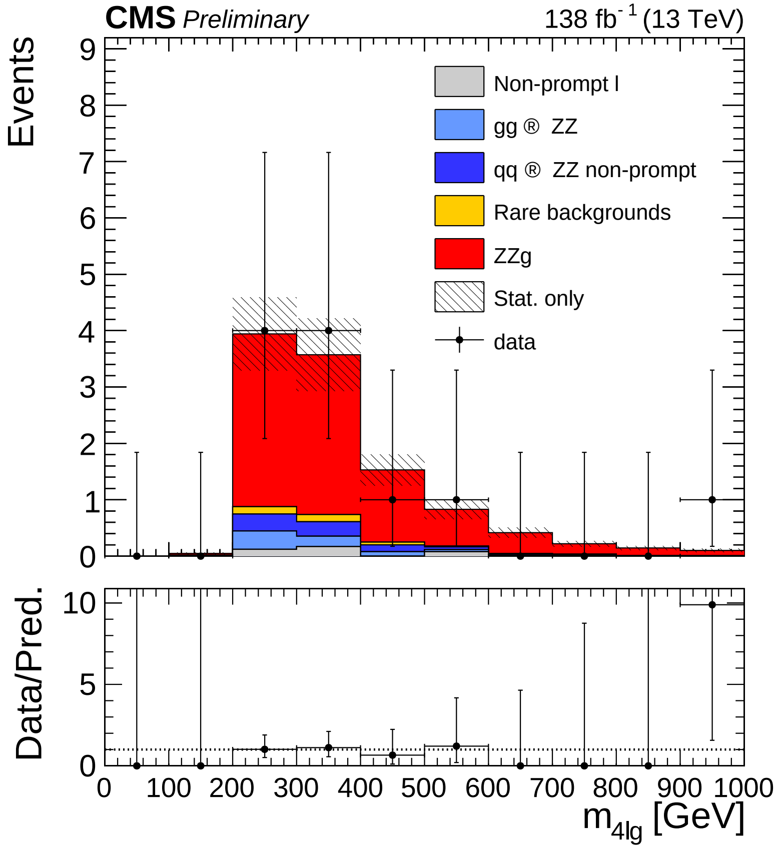

- ❑ Fit to the invariant mass of the 4 leptons + γ system
- ❑ 98 % of the total uncertainty due to statistical uncertainty
- ❑ Significance: observed 3.0 (expected 3.7) SD

$$\sigma_{\mathrm{fid}}(\mathrm{pp} \to \mathrm{ZZ}\gamma \to 4\ell\gamma)$$
$$\left[5.6^{+3.4}_{-2.8}\right] \times 10^{-2}\ \mathrm{fb}$$

Vector boson scattering in the semileptonic final state at 13 TeV

CMS-PAS-SMP-22-011 (Public since March 2025)

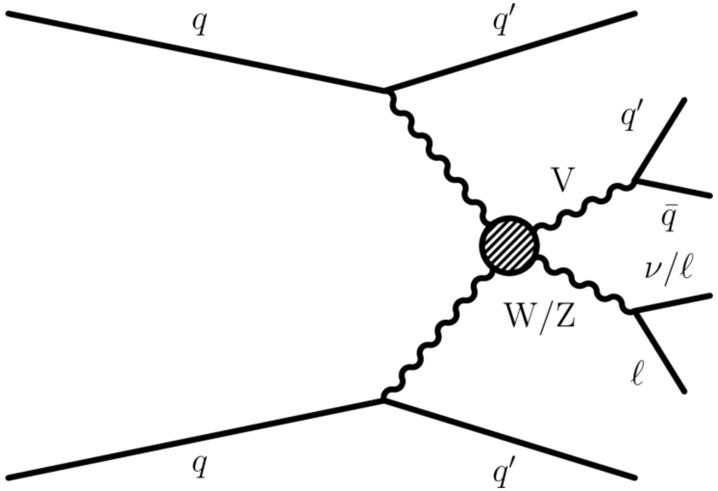

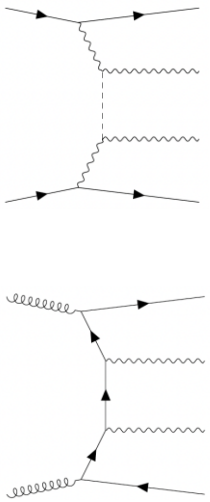

- Full RUN 2 – 138 fb^{-1}
- Semi-leptonic final state from ZV (V = W, Z) production → $l^+l^-(\mathrm{Z})q\bar{q}'(\mathrm{V})$
- The cross section measured in a fiducial region of a large invariant mass and pseudorapidity gap between the two forward jets.

- The DNN is trained to enhance the separation of the VBS EW signal from background processes dominated by Drell-Yan and single top (data driven estimations) - control regions (CRs)

- Events are categorized into two topologies to capture decays of the V boson: **boosted** and **resolved**.
  - **The boosted category** → at least one AK8 jet with a mass compatible with a W or Z boson. V decay products are highly collimated and reconstructed as a single jet
  - **The resolved category** → no AK8 jets must be present, at least two additional AK4 jets are required → Invariant mass of the jets compatible with the W or Z boson mass

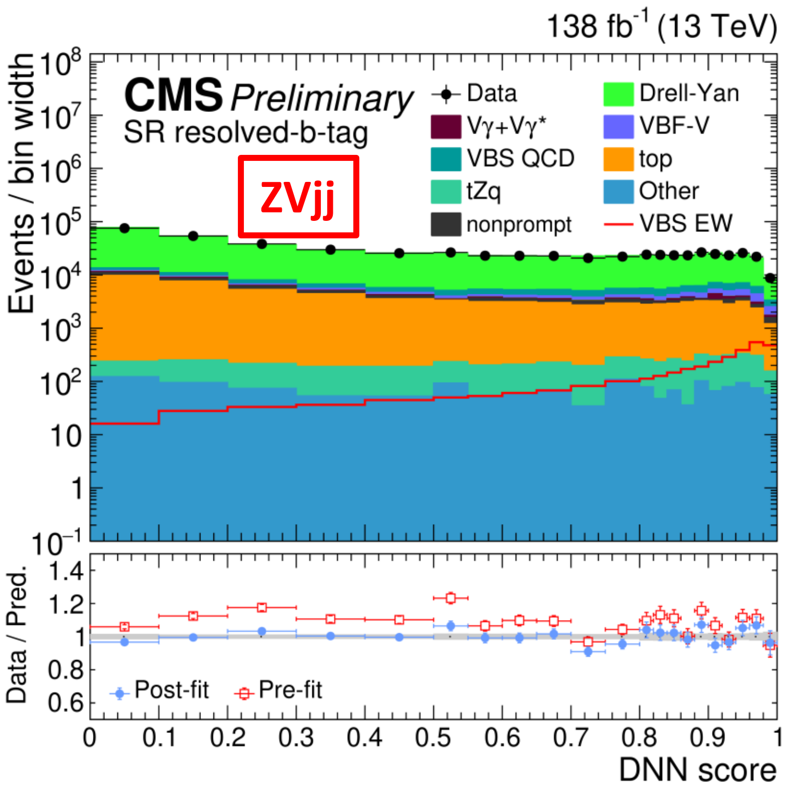

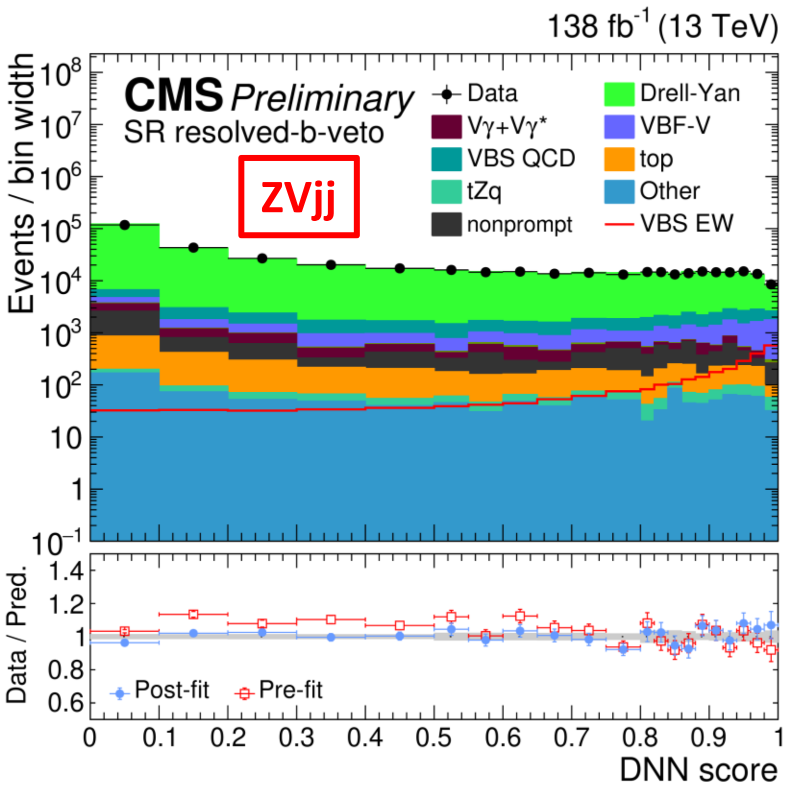

- The uncertainty dominated by statistics
- Signal strength of EW ZVjj production: $\mu_{EW} = \sigma_{obs}/\sigma_{SM} = 0.63^{+0.53}_{-0.51}$
- Observed (expected) significance 1.3σ (1.8σ)
- The ZV combined with WV semi-leptonic events → constraints on coefficients of new operators from an EFT sensitive to an anomalous electroweak production of WW, WZ, and ZZ boson pairs in association with two jets

Anomalous quartic gauge couplings are induced by 20 dimension-8 operators (backup slides)

Combination of VBS diboson measurements at 13 TeV

CMS-PAS-SMP-24-013 (Public since April 2025)

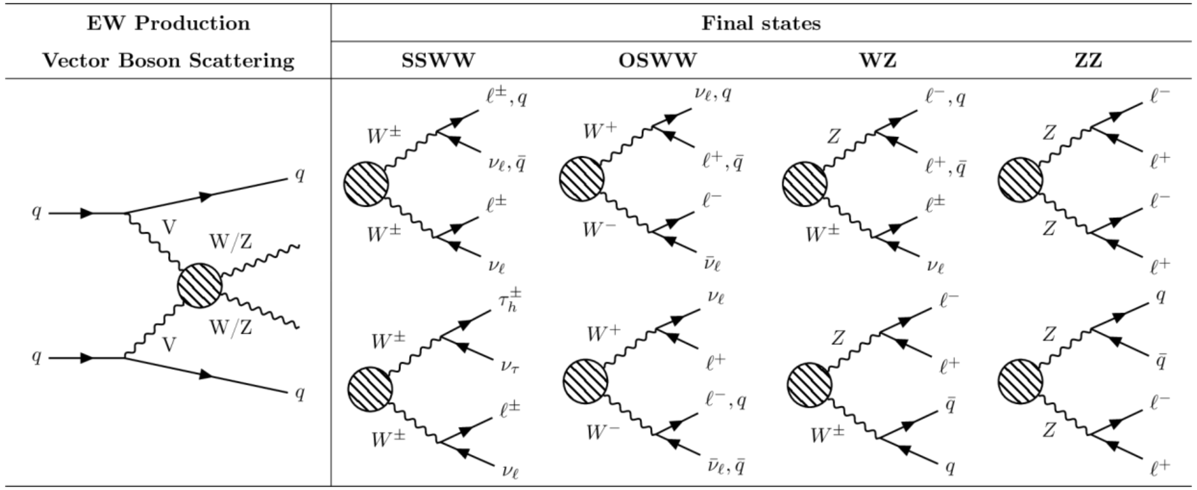

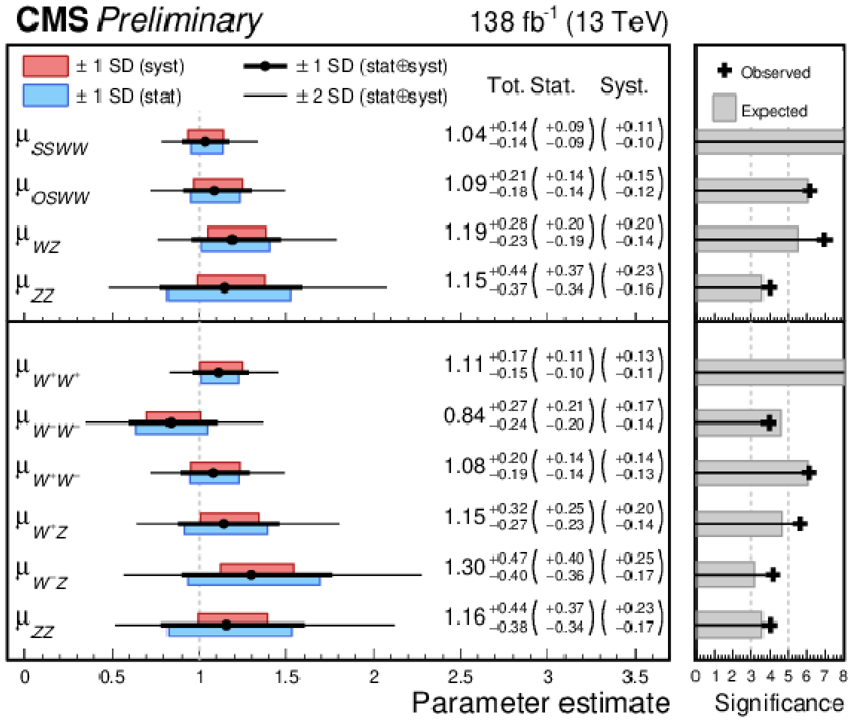

- The most comprehensive statistical combination of vector boson scattering (VBS) processes to date, integrating results from different CMS analyses

SMP-19-012 (WZ, SS WW)
SMP-20-001 (4l+2j evidence)
SMP-20-013 (WZ, WW evidence)
SMP-21-001 (OS WW observation)
SMP-22-008 (SS WW with τ)
SMP-22-011 (ZV semi leptonic)

- The results are in agreement with the Standard Model, within the uncertainty limits;

- 5-10% improvement on signal strength results

Measurement of WWZ and ZH cross sections at 13 and 13.6 TeV

CMS-PAS-SMP-24-015 (Submitted to PRL)

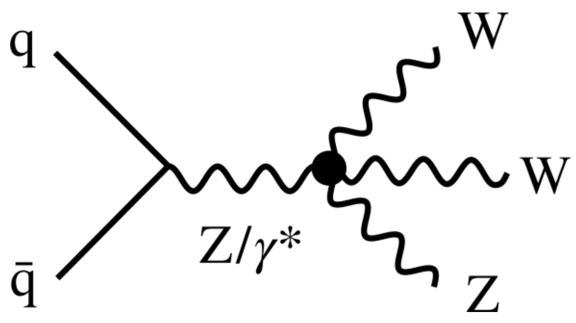

Nonresonant WWZ production

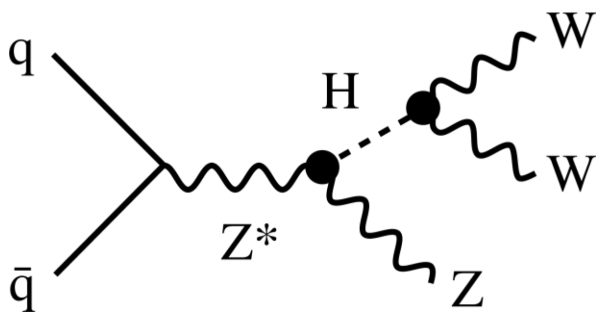

ZH production (H → W^+W^-)

- For the first time, the two processes measured separately in a simultaneous fit

  200 fb^{-1}: RUN 2 + RUN 3 (2022-2023)

→ The most precise WWZ measurement to date

→ The first measurement of tri-bosons at 13.6 TeV

- A boosted decision tree (BDT) multiclassifier is trained on signal and background MC events in order to better distinguish signal processes from background processes, and to distinguish the two signal processes from each other (backup slides)

→ The multiclassifier based on 27 event kinematic properties

- Signal regions (SRs) are then constructed by binning in the three BDT scores

- Dedicated control regions (CRs) used for estimation of the leading background contributions: ZZ, ttZ, and tWZ production.

❑ SRs and CRs are based on flavor of the charged leptons from W bosons

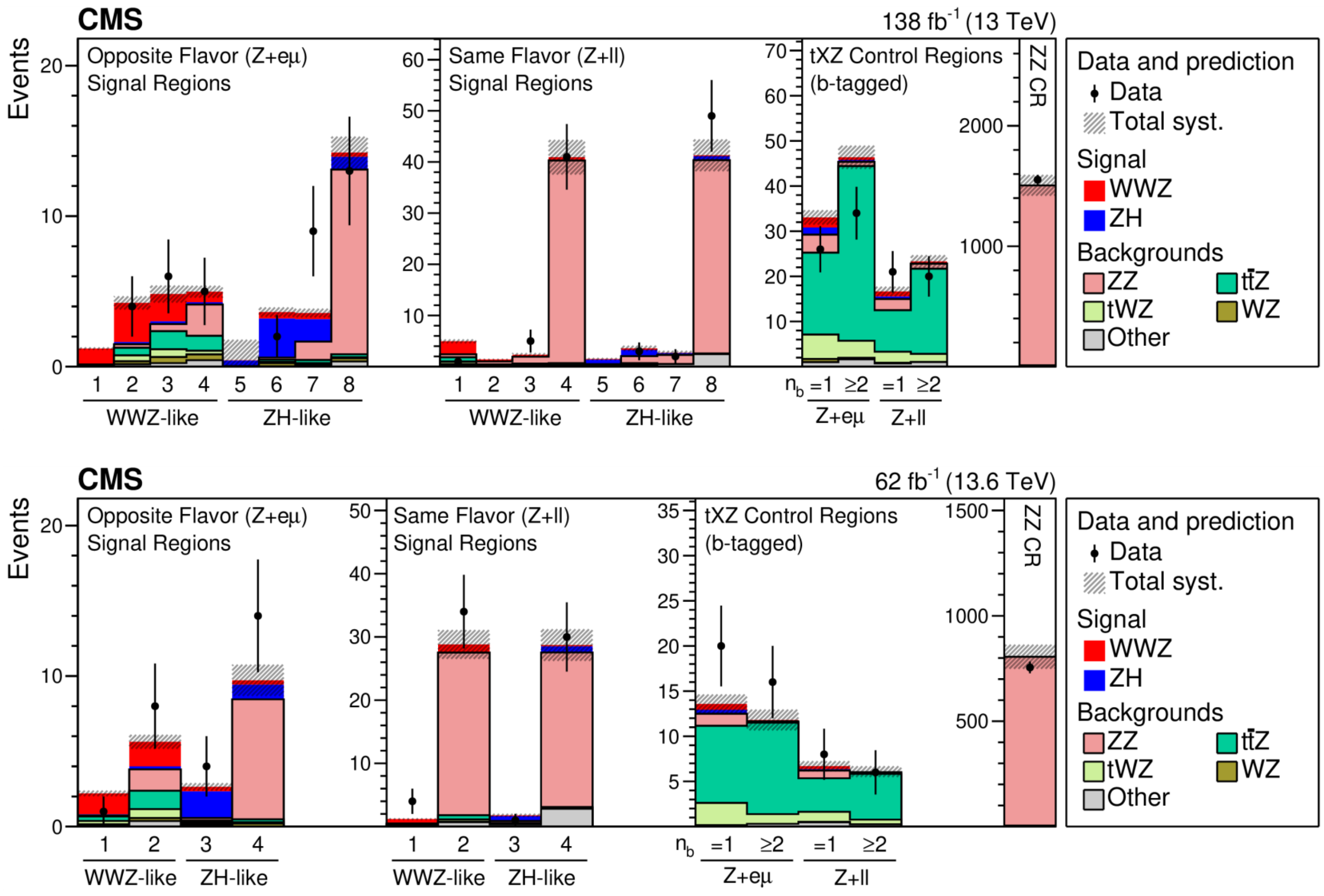

➢ The yields for signal (WWZ and ZH) and background are extracted from a simultaneous extended maximum likelihood fit to 34 bins

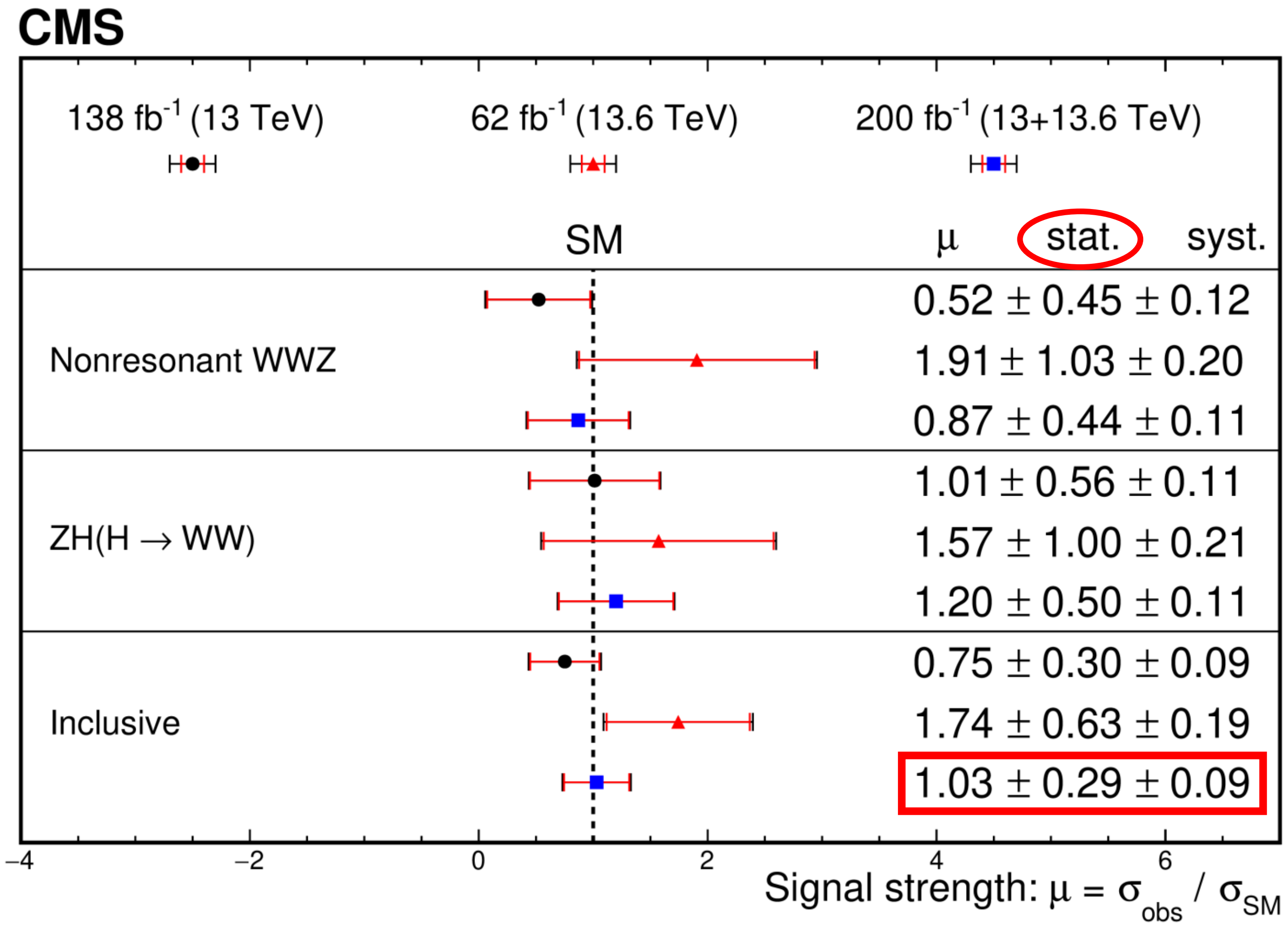

- the statistical uncertainties are much larger than the systematic ones
- systematics dominated by the BG normalization and electron ID efficiency
- the most precise measurement of WWZ production process

Era	Total	WWZ	ZH
Run 2	2.9 (4.4)	1.3 (3.1)	2.0 (2.6)
Run 3	3.8 (2.5)	2.5 (1.3)	2.5 (1.7)
Total	4.5 (5.0)	2.4 (3.3)	3.1 (3.1)

- the first evidence for triboson production at center-of-mass energy of 13.6 TeV

Summary and outlook

- ❑ CMS provides input for many aspects of understanding QCD and phenomenology
- ➢ Relaiable probes for both soft and hard phenomena across a wide range of energy scales
- ➢ Still, quite some room for better understanding and uncertainty reduction expected from the Run3

- ❑ Electroweak processes of multiboson production measured by CMS show no significant deviations from the SM, but many areas remain to be explore
- ➢ An increase of the statistics should provide more precise and new measueremnets
- ➢ Further combinations within the electroweak sector are expected to improve measurements and set tighter limits
- ➢ Application of SMEFT

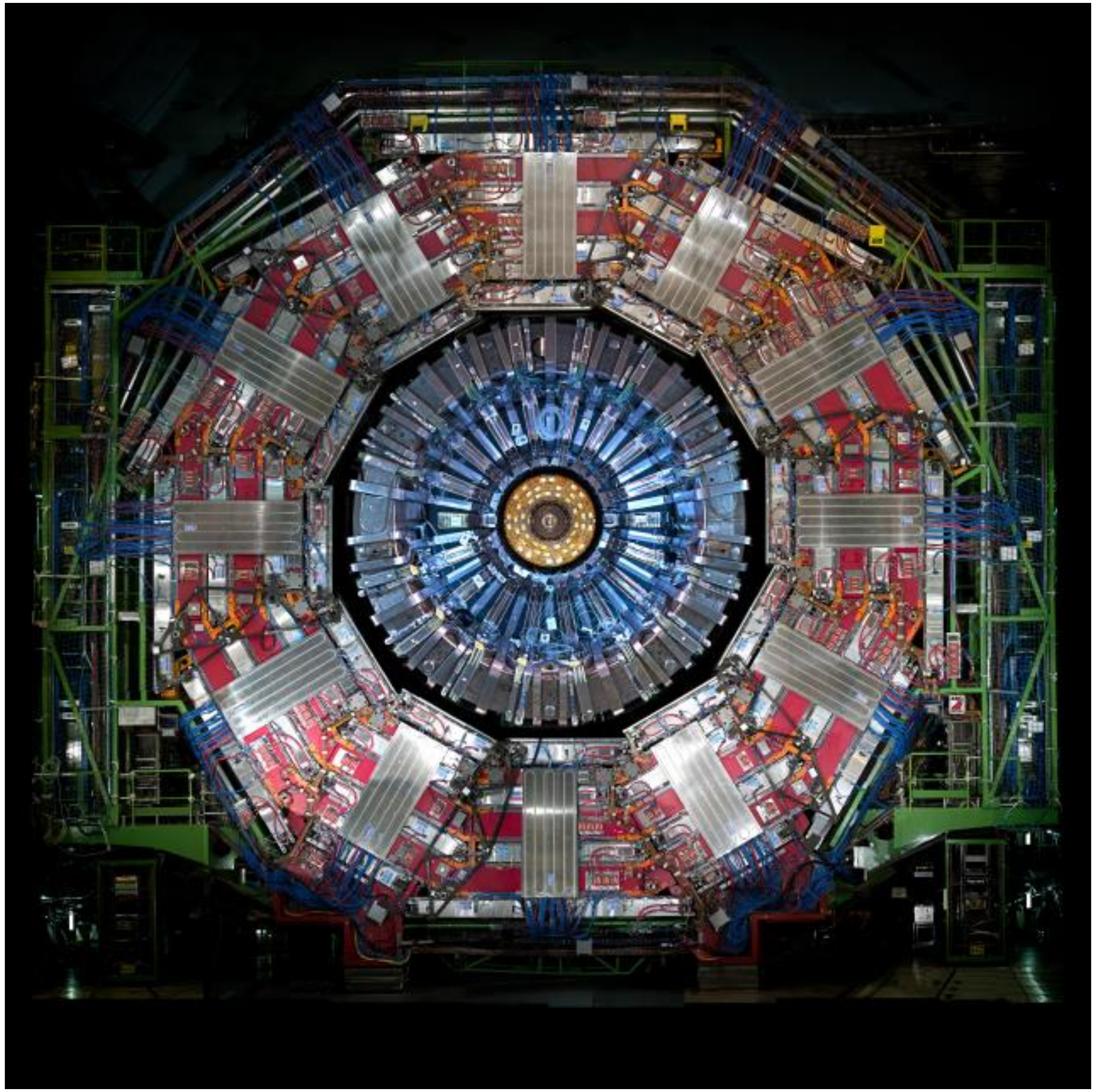

Thank you very much
for
your attention

PDFs from the simultenious fit with α_s

CMS-PAS-SMP-24-007 (Submitted to PLB)

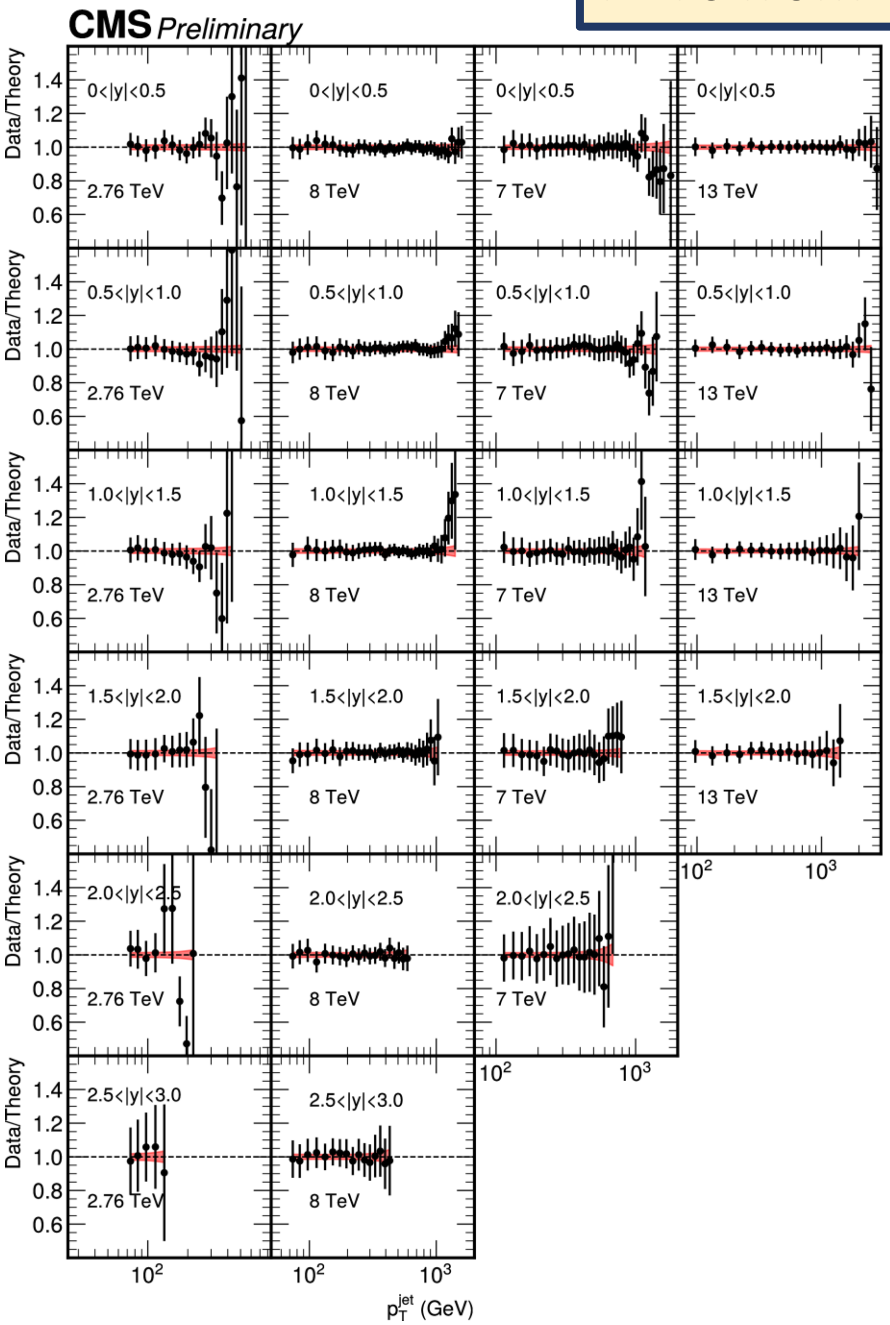

ESV from jets

CMS-PAS-SMP-22-004

- Complement of transverse thrust: the complement of transverse thrust ($\tau_\perp$) is defined as $\tau_\perp \equiv 1 - T_\perp$, where the event thrust observable in the transverse plane is defined as

$$T_\perp \equiv \max_{\vec{n}_\mathrm{T}} \frac{\sum_i |\vec{p}_{\mathrm{T},i} \cdot \vec{n}_\mathrm{T}|}{\sum_i p_{\mathrm{T},i}}$$

- Third-jet resolution parameter: defined as

$$Y_{23} = \frac{\max(p_{\mathrm{T},3}^2, [\min(p_{\mathrm{T},i}, p_{\mathrm{T},j})^2 (\Delta R_{i,j})^2 / R^2])}{P_{12}^2}$$

where i, j run over all final-state inputs and $(\Delta R_{i,j})^2 = (\eta_i - \eta_j)^2 + (\phi_i - \phi_j)^2$

- Jet broadening: in a single event one can divide the central region into two hemispheres. All particles in the upper part (U) have $\vec{p}_\mathrm{T} \cdot \vec{n}_\mathrm{T} > 0$ and in the lower part (L), $\vec{p}_\mathrm{T} \cdot \vec{n}_\mathrm{T} < 0$. The pseudorapidities and the azimuthal angles of the axes for the upper and lower event regions are defined by

$$\eta_X \equiv \frac{\sum_{i \in \mathcal{C}_X} p_{\mathrm{T},i}\, \eta_i}{\sum_{i \in \mathcal{C}_X} p_{\mathrm{T},i}}, \quad \phi_X \equiv \frac{\sum_{i \in \mathcal{C}_X} p_{\mathrm{T},i}\, \phi_i}{\sum_{i \in \mathcal{C}_X} p_{\mathrm{T},i}},$$

where X refers to the upper (U) or lower (L) side. The jet broadening variable in each region is defined as

$$B_X \equiv \frac{1}{2 P_\mathrm{T}} \sum_{i \in \mathcal{C}_X} p_{\mathrm{T},i} \sqrt{(\eta_i - \eta_X)^2 + (\phi_i - \phi_X)^2}.$$

- Jet masses: the normalized squared invariant mass of the jets in the upper and lower regions of the event is defined by $\rho_X \equiv \frac{M_X^2}{P^2}$ where MX is the invariant mass of the constituents of the jets in the region X, and P is the scalar sum of the momenta of all constituents in both sides

ESV from jets

CMS-PAS-SMP-22-004 (Public since April 2025)

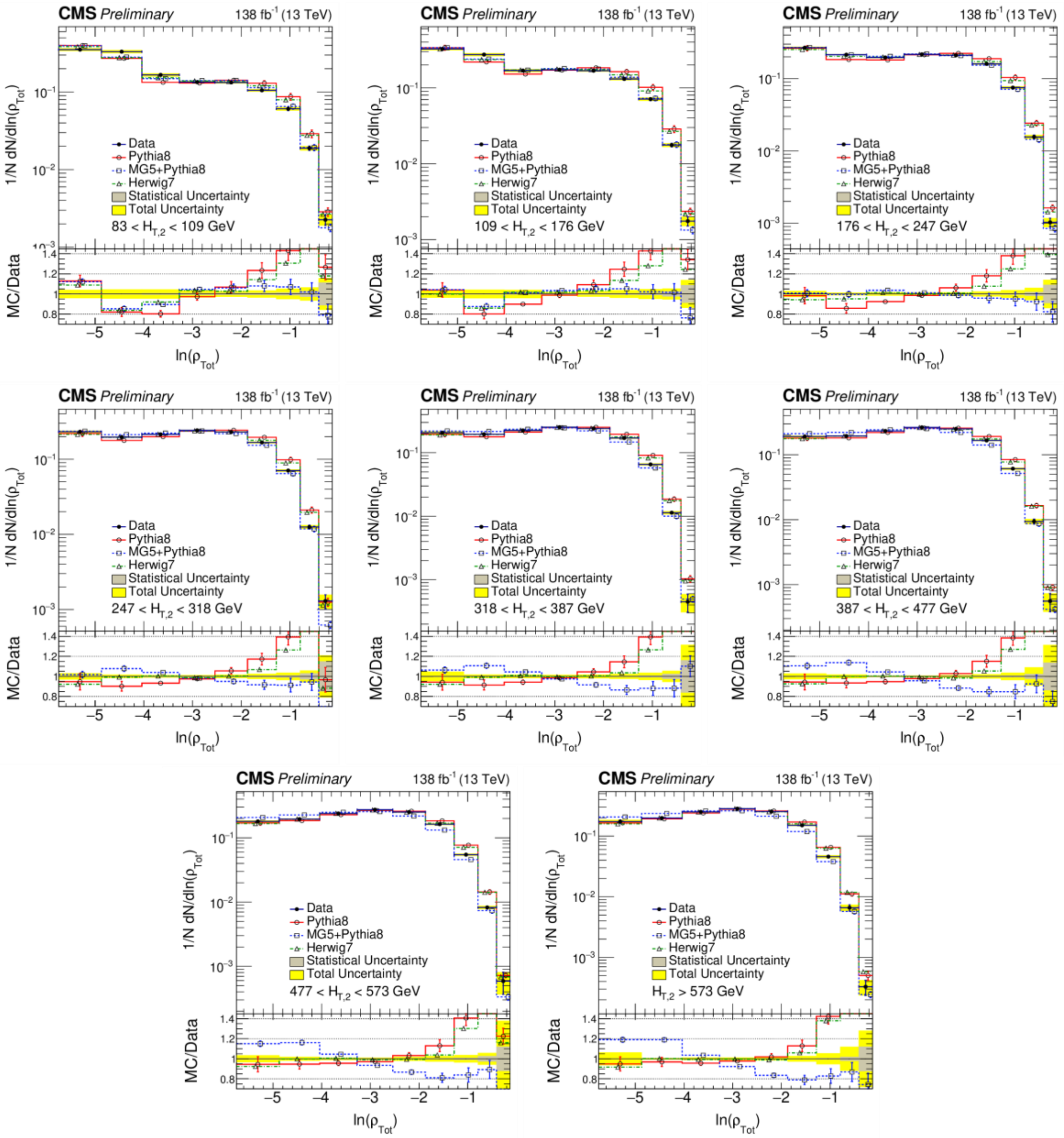

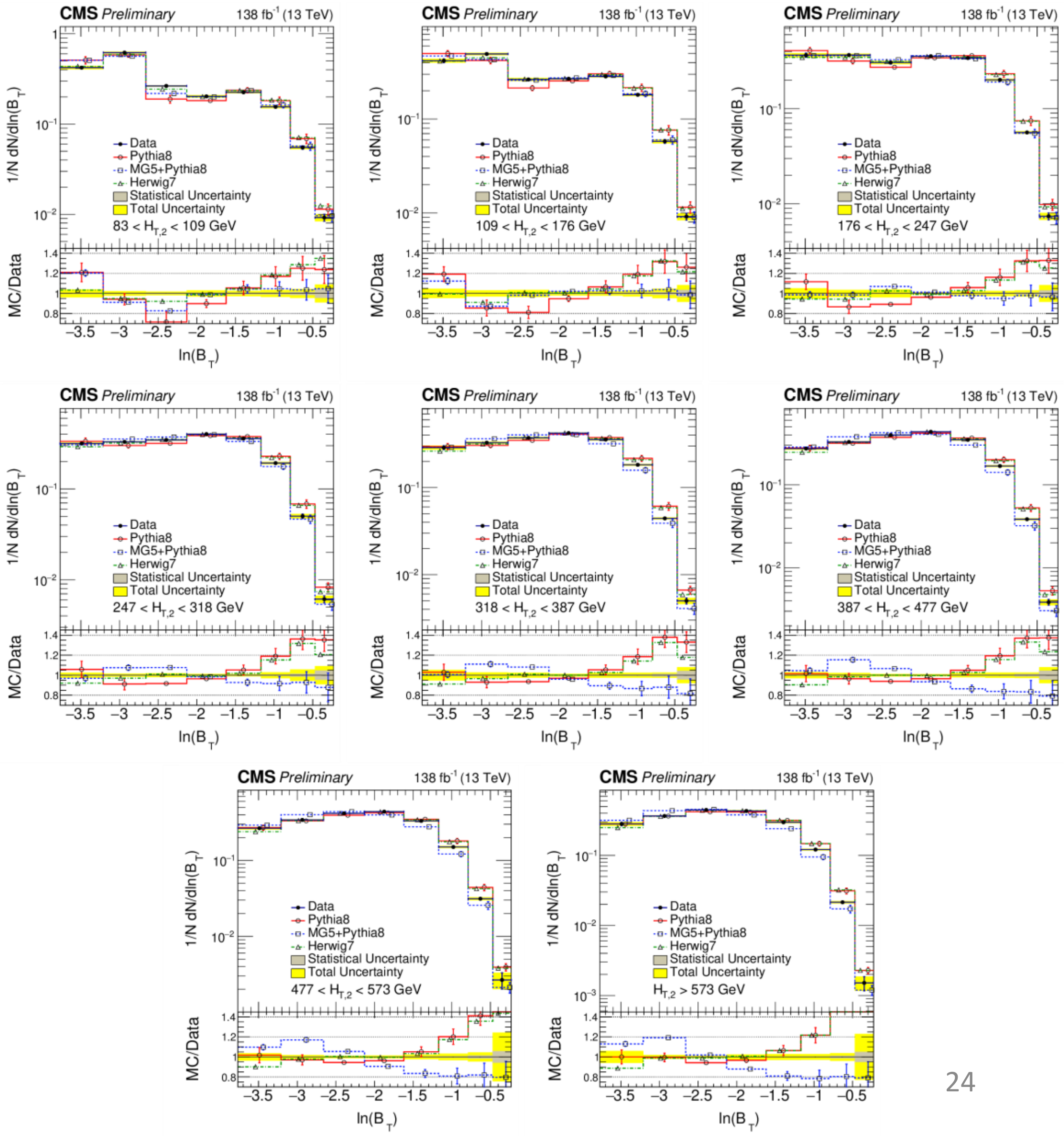

ES in minimum bias events

CMS-PAS-SMP-23-008

- Sphericity: a measure of how isotropically the momenta p are distributed in an event. The tensor S is first defined with components

$$S^{\alpha\beta} = \frac{\sum_i p_i^\alpha p_i^\beta}{\sum_i |\vec{p}_i|^2},$$

in which α, β ∈ {x, y, z} refer to Cartesian coordinates, and i is the index for the 2 final-state charged particles that passed the selections based on the detector acceptance. The sphericity is constructed from the two smallest eigenvalues λ_2 and λ_3 : S = 3/2 ($\lambda_2 + \lambda_3$).

- Broadening: a measure of the fraction of energy that is perpendicular to the thrust axis. The thrust axis defines the left L and right R hemispheres of the event. The left and right broadening are defined as

$$\mathcal{B}_{\mathcal{L}} = \sum_{i\in\mathcal{L}} \frac{|\vec{p}_i \times \vec{n}|}{2\sum_j |\vec{p}_j|}, \quad \mathcal{B}_{\mathcal{R}} = \sum_{i\in\mathcal{R}} \frac{|\vec{p}_i \times \vec{n}|}{2\sum_j |\vec{p}_j|}$$

The total broadening is the sum of the left and the righ one.

- Isotropy: a measure of how isotropically energy is distributed in an event. It is defined as the energy mover’s distance (EMD) from the spatial distribution of the tracks to a uniform radiation pattern. This variable also explores the efficacy of the isotropy to distinguish the isotropic events from the jet-like ones characterized by the majority of the transverse momentum being clustered along a few axes. For this measurement the spherical geometry was used, with the distance measure $d_{ij} = 2(1 - \cos\theta_{ij})$ where θ_{ij} is the angle between the particles.

EFT results from VBS

CMS-PAS-SMP-22-011

- Observed and expected 95% CL intervals on the parameters on the parameters of the quartic operators in WV and ZV channels. The last two columns show the observed and expected limits for the combination of the WV and ZV channels.

	Observed (WV) (TeV^{-4})	Expected (WV) (TeV^{-4})	Observed (ZV) (TeV^{-4})	Expected (ZV) (TeV^{-4})	Observed (TeV^{-4})	Expected (TeV^{-4})
f_{S0}/Λ^4	[-3.01, 3.1]	[-4.7, 4.77]	[-9.76, 9.89]	[-13.9, 14.0]	[-2.86, 2.96]	[-4.68, 4.75]
f_{S1}/Λ^4	[-4.27, 4.32]	[-6.56, 6.6]	[-10.2, 10.3]	[-13.9, 13.9]	[-3.97, 4.02]	[-6.45, 6.49]
f_{S2}/Λ^4	[-4.42, 4.48]	[-6.81, 6.86]	[-9.75, 9.89]	[-13.9, 14.0]	[-4.04, 4.11]	[-6.68, 6.73]
f_{M0}/Λ^4	[-0.568, 0.567]	[-0.844, 0.843]	[-1.38, 1.38]	[-1.74, 1.74]	[-0.539, 0.534]	[-0.828, 0.827]
f_{M1}/Λ^4	[-1.71, 1.75]	[-2.6, 2.63]	[-3.97, 4.00]	[-5.28, 5.29]	[-1.59, 1.62]	[-2.55, 2.58]
f_{M2}/Λ^4	[-0.746, 0.747]	[-1.11, 1.11]	[-1.86, 1.86]	[-2.37, 2.37]	[-0.703, 0.703]	[-1.1, 1.1]
f_{M3}/Λ^4	[-2.81, 2.81]	[-4.2, 4.2]	[-5.60, 5.59]	[-7.47, 7.47]	[-2.55, 2.55]	[-4.08, 4.07]
f_{M4}/Λ^4	[-1.74, 1.73]	[-2.6, 2.59]	[-2.70, 2.70]	[-3.61, 3.61]	[-1.48, 1.48]	[-2.42, 2.41]
f_{M5}/Λ^4	[-2.53, 2.51]	[-3.77, 3.76]	[-3.80, 3.81]	[-5.21, 5.23]	[-2.14, 2.13]	[-3.5, 3.5]
f_{M7}/Λ^4	[-2.86, 2.82]	[-4.35, 4.32]	[-6.09, 6.07]	[-8.26, 8.24]	[-2.63, 2.58]	[-4.24, 4.2]
f_{T0}/Λ^4	[-0.096, 0.083]	[-0.14, 0.128]	[-0.26, 0.25]	[-0.33, 0.32]	[-0.0921, 0.0785]	[-0.138, 0.127]
f_{T1}/Λ^4	[-0.0933, 0.1]	[-0.142, 0.149]	[-0.22, 0.24]	[-0.30, 0.31]	[-0.0863, 0.0943]	[-0.14, 0.147]
f_{T2}/Λ^4	[-0.225, 0.225]	[-0.336, 0.335]	[-0.56, 0.60]	[-0.74, 0.76]	[-0.21, 0.214]	[-0.331, 0.332]
f_{T3}/Λ^4	[-0.206, 0.206]	[-0.311, 0.31]	[-0.48, 0.51]	[-0.64, 0.66]	[-0.191, 0.194]	[-0.305, 0.305]
f_{T4}/Λ^4	[-1.09, 1.02]	[-1.58, 1.53]	[-1.44, 1.37]	[-1.84, 1.77]	[-0.895, 0.828]	[-1.4, 1.35]
f_{T5}/Λ^4	[-0.287, 0.257]	[-0.391, 0.383]	[-0.59, 0.57]	[-0.76, 0.73]	[-0.265, 0.237]	[-0.382, 0.373]
f_{T6}/Λ^4	[-0.656, 0.627]	[-0.976, 0.954]	[-0.73, 0.71]	[-0.94, 0.92]	[-0.5, 0.478]	[-0.794, 0.775]
f_{T7}/Λ^4	[-0.936, 0.899]	[-1.39, 1.36]	[-1.78, 1.67]	[-2.26, 2.16]	[-0.85, 0.8]	[-1.34, 1.29]
f_{T8}/Λ^4	–	–	[-0.53, 0.53]	[-0.67, 0.67]	[-0.53, 0.53]	[-0.67, 0.67]
f_{T9}/Λ^4	–	–	[-1.17, 1.16]	[-1.47, 1.45]	[-1.17, 1.16]	[-1.47, 1.45]

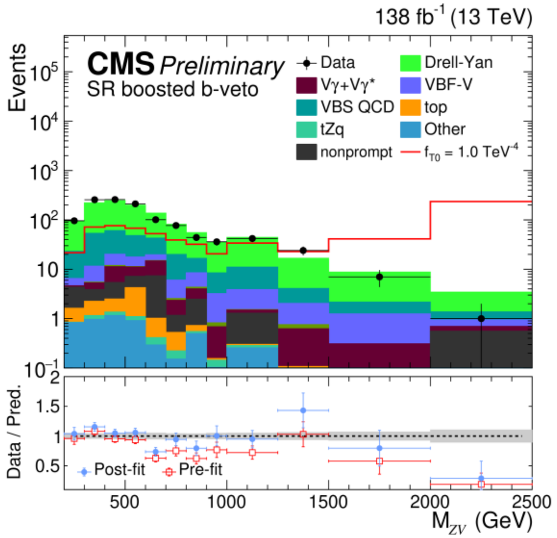

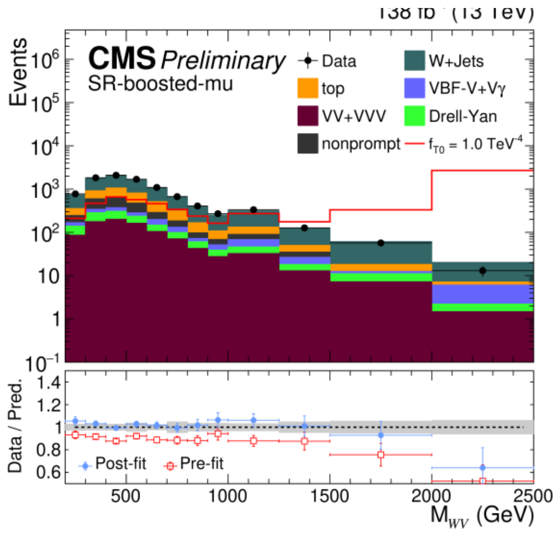

Separation of signal from background in the measurement of WWZ and ZH at 13 and 13.6 TeV

CMS-PAS-SMP-24-015

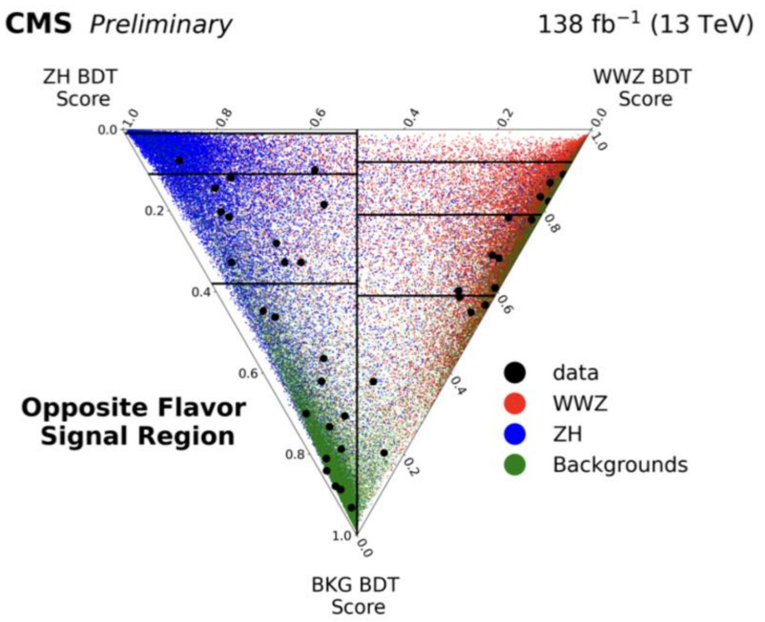

- Machine learning technique called a boosted decision tree (BDT) to further separate the signal from the remaining backgrounds. The BDT is trained on simulated data to learn to distinguish WWZ collision events from background events. The BDT is also trained to distinguish between the two different types of signal processes.

- Ternary plot showing how the BDT achieves separation between signals and backgrounds. The location of each point on the ternary plot is determined by the output scores of the BDT (which indicate how background-like, how WWZ-like, and how ZH-like each event is evaluated to be). The green points indicate simulated background processes, the blue points correspond to simulated WWZ production with an intermediate Higgs boson (i.e., ZH), and the red points indicate simulated WWZ production without an intermediate Higgs boson. The black points correspond to real data events.